TRITA-EPP-78-09

STEADY STATE MODELS FOR FILAMENTARY PLASMA STRUCTURES ASSOCIATED WITH FORCE FREE MAGNETIC FIELDS

Göran Marklund

May 1978

Department of Plasma Physics
Royal Institute of Technology
100 44 Stockholm, Sweden

STEADY STATE MODELS FOR FILAMENTARY PLASMA STRUCTURES ASSOCIATED WITH FORCE FREE MAGNETIC FIELDS

Göran Marklund
Royal Institute of Technology, Department of Plasma Physics,
S-100 44 Stockholm, Sweden

Abstract

This paper presents a model for filamentary plasma structures associated with force-free magnetic fields. A homogenous electric field parallel to the symmetry axis of the magnetic field is assumed. Under the influence of these fields, the plasma will drift radially inwards with the velocity $\underset{\sim}{v} = \frac{\underset{\sim}{E} \times \underset{\sim}{B}}{B^2}$ resulting in an accumulation of plasma in the central region. We assume recombination losses to keep the central plasma density at a finite value, and the recombined plasma i.e. the neutrals to diffuse radially outwards. Plasma density and some neutral gas density distributions for a steady state situation are calculated for various cases.

1. Introduction

In many parts of the universe we observe filamentary structures. The fine structure as well as the overall structure of solar flares and prominences can often be described in terms of filaments.

Astronomical observations show that long meandering filaments are also very frequent in interstellar and intergalactic space. These structures have been suggested to be connected with electric line currents under certain conditions, see e.g. Alfvén (1961) and also play an important role in the formation of solar systems.

In cosmical plasmas the plasma pressure is often much less than the magnetic field pressure, or

$$nkT \ll \frac{B^2}{2\mu_o} \tag{1.1}$$

Here B denotes the magnetic field strength, n the particle density and T the temperature associated with the thermal velocities of the particles.

In addition, if we assume that dynamic or gravitational forces are negligible compared with magnetic forces the inequality (1.1) above implies that the magnetic field is almost force-free and the current will flow preferentially in the direction of the magnetic field, or

$$\underset{\sim}{j} \times \underset{\sim}{B} \approx 0 \tag{1.2}$$

where $\underset{\sim}{j}$ denotes the current density.

Since filamentary structures are so common in cosmical plasmas it is of basic interest to make a general study of these, and in this paper we shall concentrate on the magmetic field, current and plasma density distributions for a general filamentary structure, under some basic assumptions.

We shall investigate the force-free case assuming a cylindrical coordinate system and an axial applied electric field. Magnetic fields, currents and motions are all axisymmetric. Under the influence of magnetic and electric fields plasma will drift radially inwards and start to accumulate in the central region. However, this accumulation of matter is limited since recombination becomes important at high densitites. The neutral gas thus produced will then diffuse outwards, see fig. 1. We shall assume

a steady state, since many observed filamentary structures can be regarded as fairly stable.

In addition to the assumptions mentioned above, force-free condition, steady state and cylindrical geometry we will use the following assumptions.

1. The ionisation rate is negligible as compared with the recombination rate within the filament.
2. Contributions to the magnetic field structure from external sources are negligible within a given radius.
3. Constant recombination rate coefficient.

Steady state implies that the typical life time, τ_o, of the filament must be much larger than the drift time for the plasma, τ_{drift}, or

$\tau_o >> \tau_{drift} = \frac{d_o B_o}{E_o}$ where d_o, $\frac{E_o}{B_o}$ are typical values of the dimension of the structure and the drift velocity of the plasma respectively. Also, energy balance within the filament requires that energy losses due to radiation and thermal conduction are at least sufficient to dissipate ohmic heating.

If the temperature is not too high, T < 6000 K, the ionisation degree can still be much larger within the filament than obtained from LTE conditions because of the inward drift of plasma.

Assumption 1 above is then valid if e.g. applying to solar prominences, with typical electron temperatures of < 6000 K or to filaments in interstellar clouds, where the electron temperature most probably is lower than this.

Between the diffuse outer surface of these filaments and the surrounding plasma there is a transition region in which temperatures, conductivities and other parameters change significantly. Also, the assumption of a homogenous electric field leads to infinite drift velocities at large distances from the axis since the magnetic field there goes to zero. However, the real magnetic field at large distances from the axis is not produced only by currents from one single filament, but also from other sources, which implies a finite magnetic field and a finite drift velocity, in the surrounding plasma.

Therefore, when treating this single filament problem we must cut off the solution at such a radius in the outer parts of the filament, that the contributions from other sources are almost negligible, see assumption 2.

Finally the recombination rate coefficient α, has a relatively weak dependence on the temperature as compared with the ionisation rate or the conductivity and we shall regard it as constant within the filament.

We consider a cylindrical coordinate system (r, ϕ, z) and calculate the ϕ and z-components of the magnetic field and current from equation (1.2) and Maxwells equation with constant electric field.

$$\underset{\sim}{\nabla} \times \underset{\sim}{B} = \mu_o \underset{\sim}{j} \qquad (1.3)$$

This gives four equations with the five unknowns B_ϕ, B_z, j_ϕ, j_z and σ, the parallel conductivity.

Since the conductivity depends on the temperature variation within the filament, but also on plasma density and perhaps also anomolous resistivity, we shall use some different approaches, with different assumptions for the conductivity. In this way we get alternative solutions, that may possibly be applied to different kinds of filaments with various dependencies on the conductivity.

In our first approach we shall give a special expression for the conductivity and then solve the above differential equations. We shall treat first the case with a constant conductivity σ_o and then the case with a varying conductivity of a form presented later.

In the second approach we shall start from a given simple expression of the total magnetic field that obeys the force-free conditions and then calculate the corresponding components of the magnetic field and current from the equations above.

2. Distribution of magnetic fields and currents

We consider an axisymmetric helical magnetic field which derives partly from currents in the plasma and partly from external sources.

$\underset{\sim}{B}(r) = (0, B_\phi(r), B_z(r))$. At the axis the magnetic field has only a z-component and is equal to B_o. A homogenous electric field is applied in the z-direction.

$$\underset{\sim}{E} = (0, 0, E_o)$$

The general pattern of the magnetic field lines, for this model is seen in fig. 2, and is often referred to as a "magnetic rope".

Case 1: Numerical solution of the magnetic field and current equations.

In the configuration considered equations (1.1) and (1.2) become

$$-\frac{dB_z}{dr} = \mu_o j_\phi \tag{2.1}$$

$$\frac{1}{r}\frac{d}{dr}(rB_\phi) = \mu_o j_z \tag{2.2}$$

$$j_\phi = |j_o|\frac{B_\phi}{|B|} = \sigma E_o \frac{B_z B_\phi}{B^2} \tag{2.3}$$

$$j_z = |j_o|\frac{B_z}{|B|} = \sigma E_o \frac{B_z^2}{B^2}, \text{ where } \sigma \text{ is the conductivity parallel to the magnetic field.} \tag{2.4}$$

Introducing in normalized variables

$$r_o = \frac{B_o}{\mu_o \sigma_o E_o} \qquad j_1 = j_z/j_o$$

$$x = r/r_o \qquad j_2 = j_\phi/j_o \tag{2.5}$$

$$y_1 = B_z/B_o \qquad \text{where } j_o = \sigma_o E_o$$

$$y_2 = B_\phi/B_o$$

$$\sigma = \sigma_o h(x), \text{ where } h(x) \text{ represents the variation.} \tag{2.6}$$

we find

$$\frac{dy_1}{dx} = - h(x) \frac{y_1 \cdot y_2}{y_1^2 + y_2^2} \tag{2.7}$$

$$\frac{dy_2}{dx} = - \frac{y}{x}^2 + h(x) \frac{y_1}{y_1^2 + y_2^2} \tag{2.8}$$

Boundary conditions at the axis are $y_1(0) = 1$, $y_2(0) = 0$

If constant conductivity is assumed in the above equations, i.e. $h(x) \equiv 1$, the solution giving the magnetic field and current is identical to that earlier given by Alfvén (1961) and Murty (1961), though obtained in a slightly different way. In the present form the solution is easy to use when later calculating the electron and neutral gas density. This case will be referred to as case 1a in the text. Next, we shall assume a vaying conductivity, which is more in agreement with a temperature variation within the filament. Consider e.g. the following function

$$h(x) = \frac{\sigma_1}{\sigma_o} = \begin{cases} \beta + \frac{1}{2}\left(1-\cos\frac{2\pi x}{3}\right) & \text{for } x < \frac{3}{2} \\ \beta + 1 & \text{for } x > \frac{3}{2} \end{cases} \tag{2.9}$$

where $\sigma_1 << \sigma_o$. This conductivity corresponds to an increasing temperature with radius, as discussed in the introduction.

<u>Case 2: Analytical solution of the magnetic field and current equations with a given analytical form of the total magnetic field.</u>

Equations (1.1) and (1.2) can also be written

$$\underset{\sim}{B} \times (\underset{\sim}{\nabla} \times \underset{\sim}{B}) = 0 \tag{2.10}$$

which in the present axisymmetric case becomes

$$\frac{d}{dr}\left(\frac{B^2}{2}\right) = - \frac{B_\phi^2}{r} \tag{2.11}$$

By introducing the following analytical form of the total magnetic field

$$\frac{B}{B_o} = \left(1 + \left(\frac{r}{r_o}\right)^n\right)^{-\frac{1}{n}} \tag{2.12}$$

We have a simple analytical expression easy to use and easy to vary through the powern. The total magnetic field B, falls off as $\frac{1}{r}$ for large distances as it should.

From the total magnetic field together with equations (1.1), (2.3), (2.4) and (2.11) we can calculate the magnetic field components and current components. In terms of the normalized variables defined by (2.5) and (2.6) we have the following result.

$$y_1 = (1 + x^n)^{-\left(\frac{1}{n} + \frac{1}{2}\right)} \tag{2.13}$$

$$y_2 = x^{\frac{n}{2}} \cdot (1 + x^n)^{-\left(\frac{1}{n} + \frac{1}{2}\right)} \tag{2.14}$$

$$j_1 = (1 + \tfrac{n}{2})\, x^{\left(\frac{n}{2} - 1\right)} \cdot (1 + x^n)^{-\left(\frac{1}{n} + \frac{3}{2}\right)} \tag{2.15}$$

$$j_2 = (1 + \tfrac{n}{2})\, x^{(n-1)} \cdot (1 + x^n)^{-\left(\frac{1}{n} + \frac{3}{2}\right)} \tag{2.16}$$

$$h(x) = (1 + \tfrac{n}{2})\, x^{\left(\frac{n}{2} - 1\right)} \cdot (1 + x^n)^{-\left(\frac{1}{n} + \frac{3}{2}\right)} \tag{2.17}$$

In fig. 3 (a,b,c,d) the magnetic field and current components are plotted for the various cases. Fig. 3a gives the solutions for the constant conductivity case.

As the figure shows, the distribution of axial magnetic field is essentially limited to a cylinder with a radius, $r_c \approx 3\, r_o$. Also the current is mainly constricted to such a cylinder and forms a line current. The B_z-field goes to zero more rapidly than the B_ϕ-field, which therefore dominates at large distances.

In fig. 3b we have plotted the corresponding solutions for the varying conductivity case. By introducing the varying condictivity we see that the axial current becomes almost zero at the axis and reaches a maximum value at a distance of about one characteristic length from the axis. The axial magnetic field as well as the ϕ-component of the magnetic field decreases more slowly than in the constant conductivity case.

For the second case with a given form of the total magnetic field, we give two different solutions, corresponding to different values of the power n, namely $n = 4$ and $n = 100$. These solutions are plotted in fig 3c and 3d respectively.

The axial component of the current has a zero value at the axis and reaches a maximum value at some distance from the axis, which is approximately equal to a characteristic length, r_o for both the cases, n = 4 and n = 100. In the former case the axial current and the magnetic field are constricted within approximately the same radius as in the constant conductivity case shown in fig. 3a. In the latter case, the current is limited to a thin cylindrical sheath with a radius of the order of r_o and a thickness of about one order of magnitude less. Between the axis and this sheath the axial magnetic field is approximately constant and equal to B_o. Then it decreases rapidly to zero outside the sheath. At large distances we have practically only a B_ϕ-component.

3. Continuity and force equations for the plasma.

The drift velocity is $\underset{\sim}{v} = \frac{\underset{\sim}{E} \times \underset{\sim}{B}}{B^2}$ or

$$v_r = - \frac{E_z B_\phi}{B^2} \quad \text{in the radial direction} \tag{3.1}$$

We normalize the drift velocity by

$$v^1 = v_r \frac{B_o}{E_o} \tag{3.2}$$

which gives

$$v^1 = \frac{y_2}{y_1^2 + y_2^2} \tag{3.3}$$

v^1 is plotted in fig. 4 for the different cases.

In case 1a v^1 shows a linear dependence on x at small and also at large distances from the axis.

For the varying conductivity case v^1 is smaller by a factor $\frac{1}{\beta}$ as compared with v^1 for the earlier case, close to the axis, but at large distance v^1 shows roughly the same dependence for the two cases.

In case 2, v^1 is exactly linear for n = 2 but with an increasing n, v^1 becomes smaller and smaller close to the axis and at large distances, it is approximally proportional to x.

Recombination is the dominating loss process for the plasma and the neutral gas produced diffuses radially outwards.

Since v_e is not constant there is also a dynamic pressure acting on the plasma. However, for this pressure to exceed the gas pressure the drift velocities have to be greater than the thermal velocities, which is definitively not the case, so the force free picture is still valid.

The force-free condition means that the plasma motion is totally determined by the magnetic field and the electric field, while the neutrals move independently of these fields. The pressure gradient of the neutrals balances the frictional forces between the two opposite motions.

The continuity equations for the electron gas and the neutrals in the plasma are then with the following notation

n_e = electron density

n_n = neutral gas density

v_e = electron and ion drift velocity

v_n = neutral gas diffusion velocity

v_{ith} = ion thermal velocity

m_n = mass of neutral particle

σ_c = total atomic cross section (elastic and inelastic)

α = recombination coefficient

$$\frac{\partial n_e}{\partial t} = -\alpha n_e^2 - \underset{\sim}{\nabla} \cdot (n_e \underset{\sim}{v_e}) \qquad (3.4)$$

$$\frac{\partial n_n}{\partial t} = +\alpha n_e - \underset{\sim}{\nabla} \cdot (n_n \underset{\sim}{v_n}) \qquad (3.5)$$

Force-balance for the neutral gas

$$\frac{dP_n}{dr} = m_n n_n (v_n - v_e) n_e \sigma_c \langle v_{ith} \rangle \qquad (3.6)$$

4. Plasma density profile

In steady-state and cylindre geometry equation (3.4) becomes

$$\frac{dn_e}{dr} + \frac{1}{rv_e} \frac{d}{dr} (rv_e) n_e = -\frac{\alpha}{v_e} n_e^2 \qquad (4.1)$$

We introduce $n^* = n_e/n_o$ where n_o is a typical density with which we normalize the density variables and $K = \frac{\alpha r_o B_o n_o}{E_o}$, , (4.2)

Equation (4.1) can be written

$$\frac{dn^*}{dx} + \frac{1}{xv^1} \cdot \frac{d}{dx}(xv^1)n^* = \frac{K}{v^1} \cdot n^{*2} \qquad (4.3)$$

or in terms of the normalized components of the magnetic field.

$$\frac{dn^*}{dx} + \frac{1}{1+(y_2/y_1)^2} \cdot \frac{2(y_2/y_1)^2}{x} + \frac{h(x)}{y_2} n^* = K \cdot \frac{y_1^2}{y_2}(1+(y_2/y_1)^2)n^{*2} \qquad (4.4)$$

The normalized plasma density, n^* is then calculated by integration of this equation.

1a : Electron density distribution for the constant conductivity case

For small x, $x \ll 1$ we get

$$y_1 \simeq 1 - \frac{x^2}{4}$$

$$y_2 \simeq \frac{x}{2}$$

$$v^1 \simeq \frac{x}{2}$$

If we insert this value for v^1 in equation (4.3) this can be integrated and we get

$$n^* = \frac{1}{K - Ax^2} \quad \text{(where A is an integration constant)} \qquad (4.5)$$

This gives $K = \frac{1}{n^*(o)} = \frac{n_o}{n_e(o)}$ (4.6)

Since $K = \frac{\alpha r_o B_o n_o}{E_o}$ we obtain the density at the axis as

$$n_e(o) = \frac{E_o}{\alpha r_o B_o} = \frac{\mu_o \sigma_o E_o}{\alpha B_o^2} \qquad (4.7)$$

i.e. with a given electric field, recombination coefficient, conductivity and magnetic field, the density at the axis is given independently of boundary conditions.

1b: Electron density distribution in the varying conductivity case.

If one permits the conductivity to vary between a low value in the centre and a higher value further out we ought to get a pronounced density peak away from the axis since the drift velocity then is low close to the axis. Using the conductivity function in equation (2.9) we get for small x:

$$y_1 \simeq 1$$

$$y_2 \simeq \frac{\beta x}{2}$$

$$v^1 \simeq \frac{\beta x}{2}$$

Integrating equaion (4.3) as before with the above approximation for v^1 gives

$$n^* = \frac{1}{\frac{K}{\beta} - Ax^2} \qquad (4.8)$$

which should be compared with equation (4.5)

$$K = \frac{\beta}{n^*(o)} = \frac{n_o}{n_e(o)} \cdot \beta \qquad (4.9)$$

Using (4.2) we get

$$n_e(o) = \frac{\beta E_o}{\alpha\, r_o\, B_o} \qquad (4.10)$$

The axial density is thus reduced with the factor $\frac{1}{\beta}$ as compared with the constant conductivity case.

2: Electron density distribution for the analytical case with a given total magnetic field

The normalized drift velocity v^1 defined in equation (3.3) will now be

$$v^1 = x^{\frac{n}{2}} (1 + x^n)^{-(\frac{1}{2} - \frac{1}{n})} \quad \text{see fig. 4} \qquad (4.11)$$

For small x the drift velocity is

$$v^1 \simeq x^{\frac{n}{2}}$$

Integrating (4.3) as before gives the density close to the axis

$$n^* = \frac{x^{\frac{n}{2}-1}}{\frac{K}{n} - Ax^n} \simeq \frac{n}{K} x^{\left(\frac{n}{2}-1\right)} \tag{4.12}$$

The maximum density is

$$n^*_{max} = \frac{1}{K} \frac{(\frac{n}{2}+1)x^{-n+2}}{(1+x^{-n})^{\frac{3}{2}-\frac{1}{n}}} = \frac{1}{K} a_n(x) \tag{4.13}$$

The largest peak value for a given n occurs for

$$x = \left(\frac{\frac{n^2}{4} - 1}{\frac{n^2}{2} - 2n+2}\right)^{\frac{1}{n}} \tag{4.14}$$

In the figures 5, 6, 7 and 8 we have plotted the normalized electron density distributions, as calculated from equation (4.4) for the various cases. For each case we have given some various density profiles corresponding to different boundary conditions and also the locus for various maximum (dotted lines). The densities are all normalized with $n_o = \frac{E_o}{\alpha\, r_o\, B_o}$, equal to the axial density for the constant concuctivity case.

In fig. 5 we see the solutions for the constant conductivity case. As the figure shows a serie of different distributions of varying form and radial dimension corresponding to different boundary conditions for n_e are possible.

Since we have not included the plasma density value at large distances, $n_e\ (\infty)$, in our calculation these series of curves can be used to fit in various cases corresponding to different ratios

$$\frac{n_e\ (\infty)}{n_e\ (o)} .$$

In fig. 6 we have the corresponding normalized electron density profiles for the varying conductivity case.
For the bounded solutions we can now get peak densitites about $\frac{1}{\beta}$ times larger than the central value. The low density in the centre is consistent with the low drift velocities, which is a consequence of the low conductivity there.

The solutions for the analytical case are given in the figures 7 and 8, corresponding to n = 4 and n = 100.

For n = 4 we get bounded solutions for normalized peak densities smaller than 2 and for n = 100 normalized peak densities smaller than approximately 7.

In fig. 8 we have enlarged the scale for x in order to make a closer study of the narrow region around the peaks. We have a cylindrical sheath of plasma with a thickness of about 0.1 r_o and a radius around r_o.

The differences between the density profiles for the various cases can be understood by looking at the corresponding drift velocities. Far from the axis all drift velocities are approximately linear with x. Close to the axis the drift velocities are approximately linear with x in case 1a and 1b but because of the low conductivity in the latter case the drift velocity becomes $\frac{1}{\beta}$ times slower. The plasma will therefore not have enough time to reach the central region within the lifetime of the filament. This is the same for case 2 where the drift velocity is $v^1 \propto x^{n/2}$.

In the intermediate region the drift velocities change more or less abrubtly. For case 1b and case 2 the high derivates of the drift velocity means that there is a large compression rate responsible for the pronounced peaks. In case 1a the compression rate is not very much different from that in the centre resulting in relatively flat distributions.

5. Neutral gas density profile

If we use equation (3.6) and the neutral gas density

$P_n = n_n kT$, we get (5.1)

$$\frac{dn_n}{dr} = - \frac{m_n \sigma_c}{kT} n_n n_e \langle v_{ith} \rangle (v_n - v_e) \tag{5.2}$$

Adding equation (3.4) and (3.5) and requiring finit values at the axis gives

$$n_n v_n = - n_e v_e \qquad (5.3)$$

Together with (5.2) we have

$$\frac{dn_n}{dr} = - \frac{m_n \sigma_c}{kT} n_n n_e \langle v_{ith} \rangle \left(- \frac{n_e v_e}{n_n} - v_e \right) \qquad (5.4)$$

We introduce $n_n^* = n_n / n_{no}$, where n_{no} is a typical neutral gas density, and use the relations (2.7)

$$\frac{dn_n^*}{dx} + \left[A' n_e^* (*v') \right] n_n^* = - \left[B' n_e^{*2} (*v') \right] \qquad (5.5)$$

where

$$A' = \frac{m_n}{kT} \sigma_c n_o r_o \left(\frac{E_o}{B_o} \right) \langle v_{ith} \rangle$$

$$B' = A' \frac{n_o}{n_{no}}$$

Integrating this equation gives the density distributions for tne neutral gas.

Thé values within the brackets in equation (5.5) are both positive and therefore the neutral density profiles do not include any maxima away from the axis. In order to get a better feeling for how the neutral gas density profiles look we shall first give values of A' and B' defined above, and then solve equation (5.5) using the normalized electron density function, n^*, for the constant conductivity case, (see fig.5). With typical prominence data, wee get the distributions, seen in fig.9. The different curves correspond to different choices of boundary conditions for n^*. A flat electron density distribution gives a steep and narrow neutral gas density distribution, and the reverse situation with a steep and narrow electron density distribution gives a flat neutral gas density distribution.

For the other cases, case1b and case 2, we shall very briefly discuss the general picture for these density profiles. Since here the values of the electron density and the drift velocity,

are very low in the central region, the terms within both the brackets of equation (5.5) are negligible.

This gives us $n_n^* \simeq 1$ for $x \ll 1$

Far from the axis we want the ratio between plasma density and neutral gas density to be larger than in the centre. In other words the ionization degree ought to increase as we go outwards since the filament is embedded in a highly ionized plasma.

In terms of n^* and n_n^* this can be expressed

$n^*(x) > n_n^*$ for $x \gg 1$.

As can be seen in equation (5.5) the right hand term will determine the equation at large distances from the axis. However the densities has here gone down significantly from the central value and therefor one could assume the recombination to be negligible giving

$\mathrm{div}(n^* v^1) \simeq 0$ or $n^* \times v^1 = \text{const.}$

Since v^1 is proportional to x we get

$n^* \propto \frac{1}{x^2}$

If we put this into equation (5.a)

$\frac{dn_n^*}{dx} \propto -\frac{1}{x^3} \quad \because \quad n_n^* \propto \frac{1}{x^2}$

In the intermediate region where the plasma density reaches its maximum the terms within the brackets of equation (5.5) will be large, giving a strong negative gradient of the neutral gas density distribution. This is needed to balance the large frictional forces between plasma and neutrals, which is a consequence of the high compression there. Cases that give very pronounced plasma density peaks will result in a very strong gradient for the neutral gas distribution.

The general picture will then be something like in fig.10

7. Discussion

We have thus given some alternative forms of the plasma density distribu ions, assuming diff rent conductivity variations for a filament associated with force free magnetic fields. Instead of assuming a conductivity one could use the energy balance equation to derive a temperature variation by which the conductivity can be determined and thus close the system of equations. The temperature can be deduced from the balance between ohmic heating, transport of energy by the plasma from the surroundings and coolin by radiation. To close this system of equations we have to consider very special and well defined cases, and still such a solution is very uncertain, since it depends critically on the boundary conditions used. Secondly the Spitzer conductivity might not be applicable to the filament plasma.

Since the conductivity surely varies within the filament as well as between different filaments our aim was, by choosing these different conductivity functions to try to cover some of the various situations.

In this particular model we arrived at an expression for the axial plasma density, n_o, in the constant conductivity case, see equation (4.7). Using the expression for the characteristic length, r_o, defined in (2.5), the conductivity σ_o, required for a particular set of values of n_c, r_o, and a is

$\sigma_o = (n_c\, r_o^2\, \mu_o\, a)^{-1}$. From this we see that an increase of the conductivity by two orders of magnitude requires for example a decrease of the characteristic length by one order of magnitude, given that the other parameters are fixed.

In the present form this model is applicable to a single competent plasma. When considering a multicomponent plasma we can no longer neglect the ionisation effect, since with different ionisation potentials of the elements, some of these may be almost fully ionised and others neutral at the same radius. Assuming a positive temperature gradient $\frac{dT}{dr} > 0$, due to e.g. a preferential cooling by radiations of the densest plasma regions, (which may correspond to case 1b above, where we had assumed a positive conductivity gradient, $\frac{d\sigma}{dr} > 0$) we will get a chemical separation of the elements into successive coaxial regions, due to tne different ionisation potentials.

Elements with high ionisation potential will recombine predominantly in the outer parts of the filament where the temperature is relatively high, while elements with low ionisation potential will recombine and accumulate in the central regions. Diffusion of the neutrals, with different diffusion rates, will alter the steady state distribution, so as to smear out the boundaries between these regions. Also, the distribution will be dominated by those elements with high relative abundancies, such as hydrogen and helium.

The next step will thus be to to make a quantitative analysis of the multicomponent plasma case taking into account different diffusion rates of the elements and make applications to the various filamentary structures observed.

Acknowledgements

The author is indebted to Prof. H. Alfven for suggesting this problem,and for many fruitful discussions. Special thanks also to Prof. C.G. Fälthammar, Dr. M. Raadu and Dr. P. Carlquist for valuable discussions and suggestions for improvements and to Mrs. K. Forsberg for the drawings.

References

Alfvén, H.: 1961, "Filamentary Structures produced by an Electric Current in a Plasma, Ark..f..Fys. 19, 375.

Jefferies, J.T. and Orrall, F.Q.: 1963, Astrophys. J. 137, 1232.

Mouradian, Z. and Leroy, J.L.: 1976, Solar Phys, 51, 103.

Murty, G.S.: 1961, "Filamentary Structure associated with Force free Magnetic Fields", Ark. f. Fys. 21, 203.

Tandberg-Hanssen, E.: 1974, Solar Prominences, D. Reidel Publishing Company, Dordrecht-Holland/Boston-U.S.A.

Figure Captions

Fig 1. General picture of the model. Plasma density profiles are sketched qualitatively for the case of no recombination, recombination with constant conductivity and recombination with low central conductivity

Fig 2. General form of the magnetic field line pattern in the filament

Fig 3 a,b,c,d Magnetic field and current distribution given in a normalized form using

$$y_1 = B_z/B_o,\ y_2 = B_\phi/B_o,\ j_1 = j_z/j_o,\ j_2 = j_\phi/j_o$$

Fig 3a. Case 1a with constant conductivity

Fig 3b. Case 1b with varying conductivity

Fig 3c. Case 2, with n=4

Fig 3d. Case 2, with n=100. The scale is here enlarged around x=1, where the variables change rapidly

Fig 4. Absolute value of the radial drift velocity for the different cases.
Curve
I ;case 1a
II ;case 1b
III;case 2 using n=4
IV ;case 2 using n=100

Fig 5, 6,7,8 Normalized plasma density distributions corresponding to different boundary conditions for the various cases $n^* = n_e/n_o$ where

$$n_o = \frac{E_o}{\alpha r_o B_o}$$

The dotted lines represents all the possible maxima for the different solutions

Fig 5. Case 1a

Fig 6. Case 1b

Fig 7. Case 2 with n=4

Fig 8. Case 2 with n=100

Fig 9. Normalized neutral gas density distributions, $n_n^* = n_n/n_{no}$, for the constant conductivity case, calculated by use of typical prominence data.
The different curves are calculated for n^* distributions with various boundary conditions.
Curve I corresponds to an electron density distribution of about the same radial dimension as the magnetic field distribution, curve II and curve III correspond to flatter and broader distributions than used for curve I

Fig 10. Schematic picture of the normalized neutral gas density distributions for the various cases.
curve I corresponds to case 1b and case 2 with n=4
curve II corresponds to case 1a
Curve III corresponds to case 2 with n=100

Fig. 1

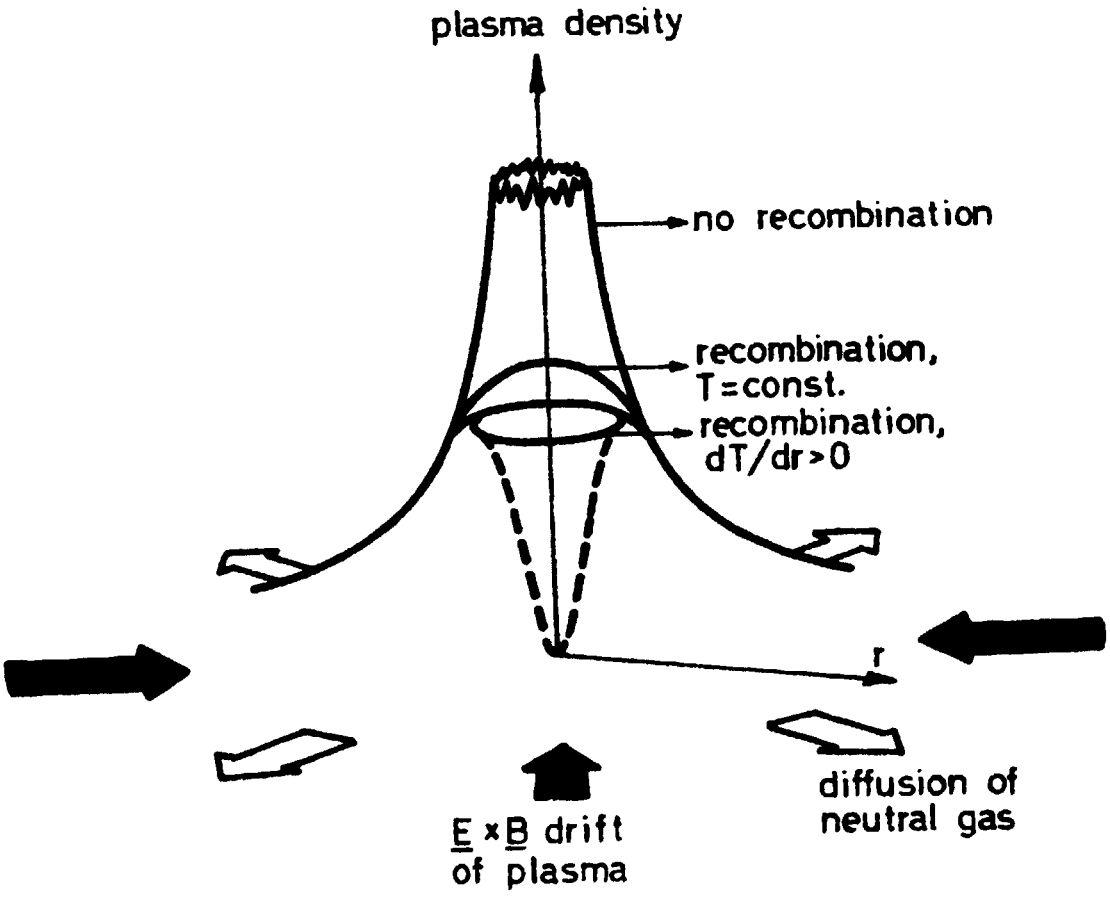
plasma density
no recombination
recombination,
T=const.
recombination,
dT/dr>0
r
E x B drift
of plasma
diffusion of
neutral gas

Fig. 2

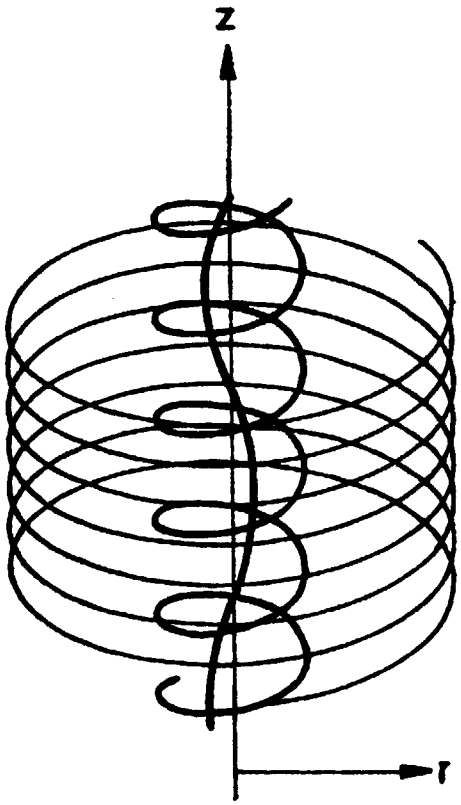

Fig. 3a

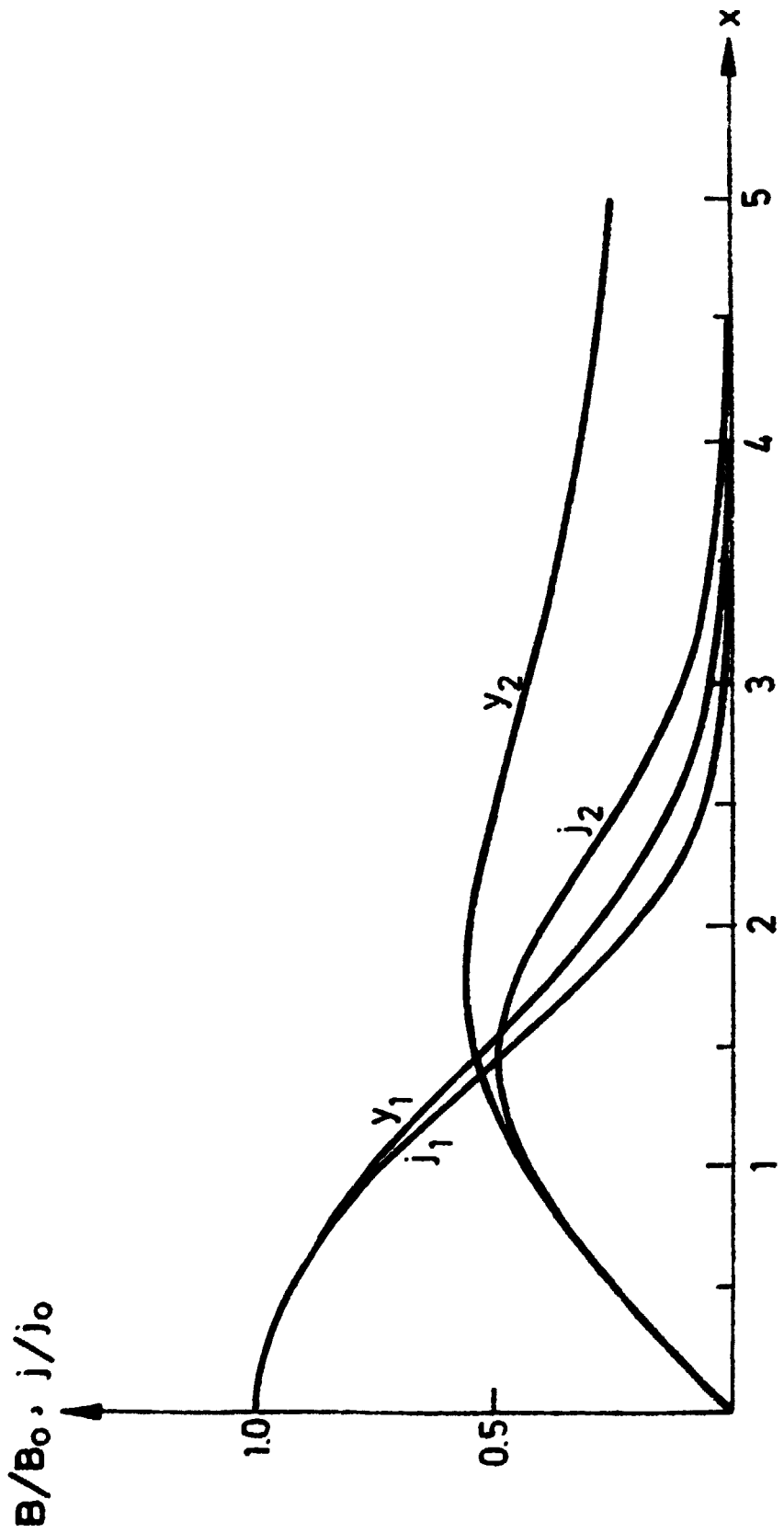

Fig. 3b

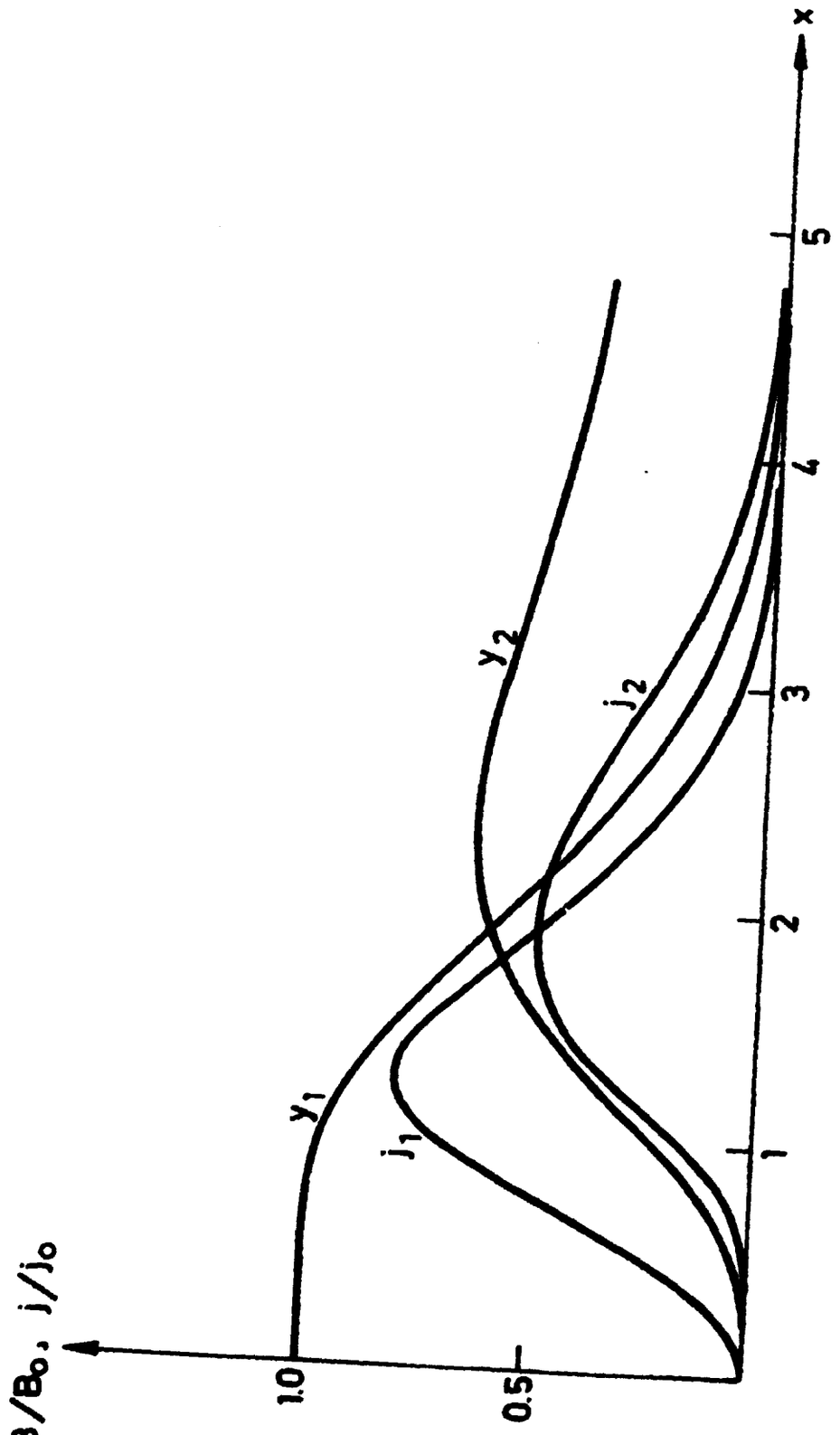

Fig. 3c

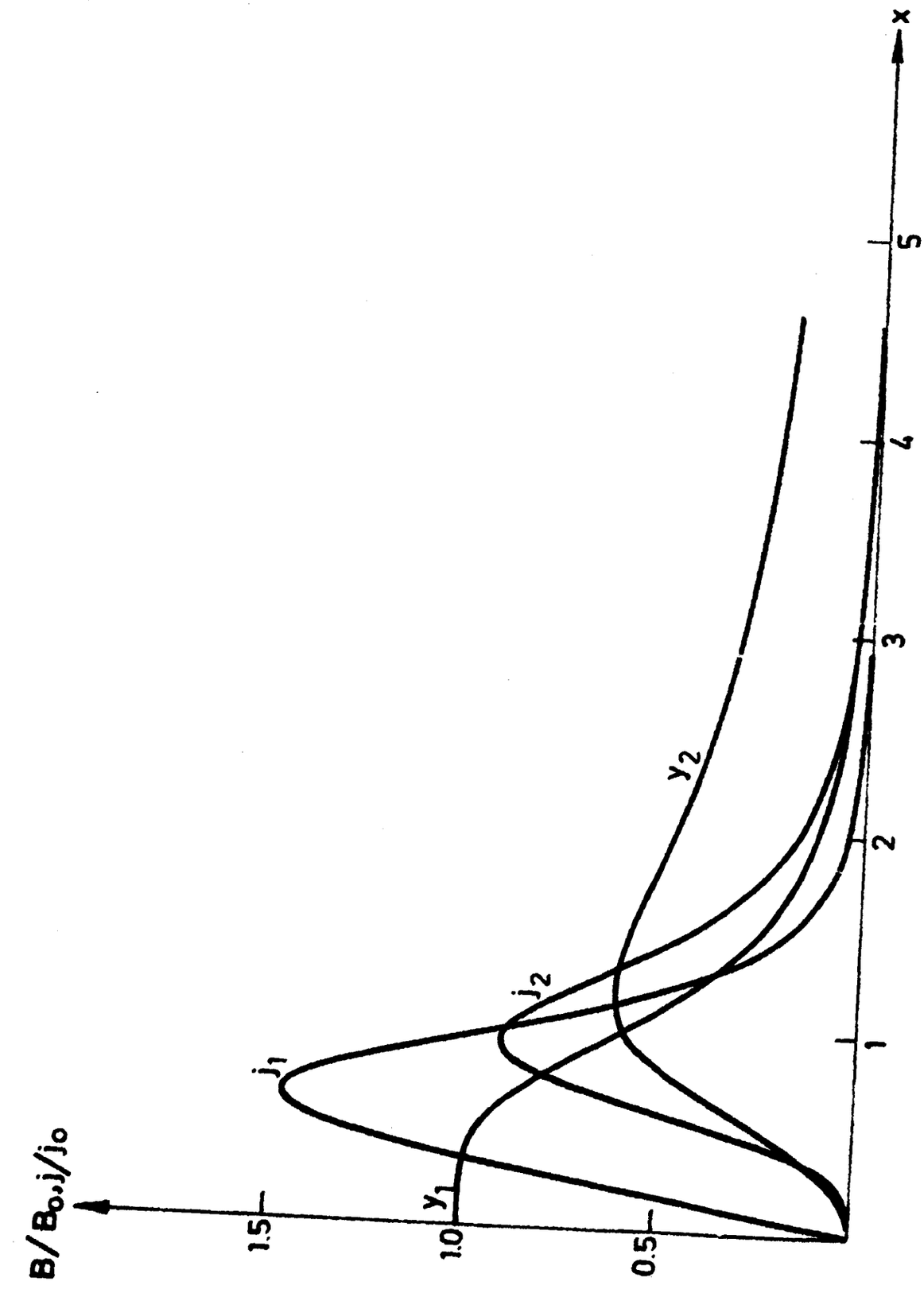

Fig. 3d

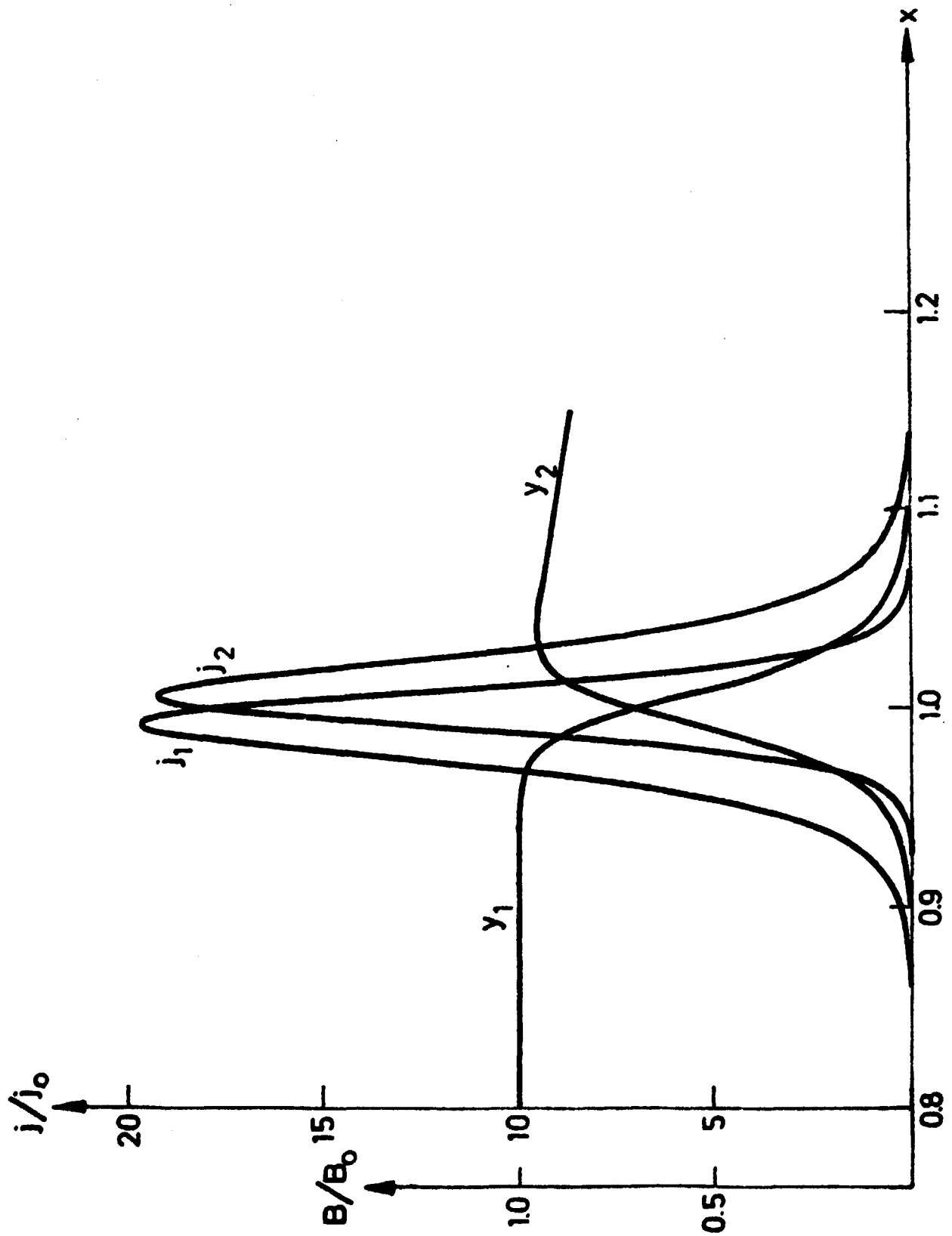

Fig. 4

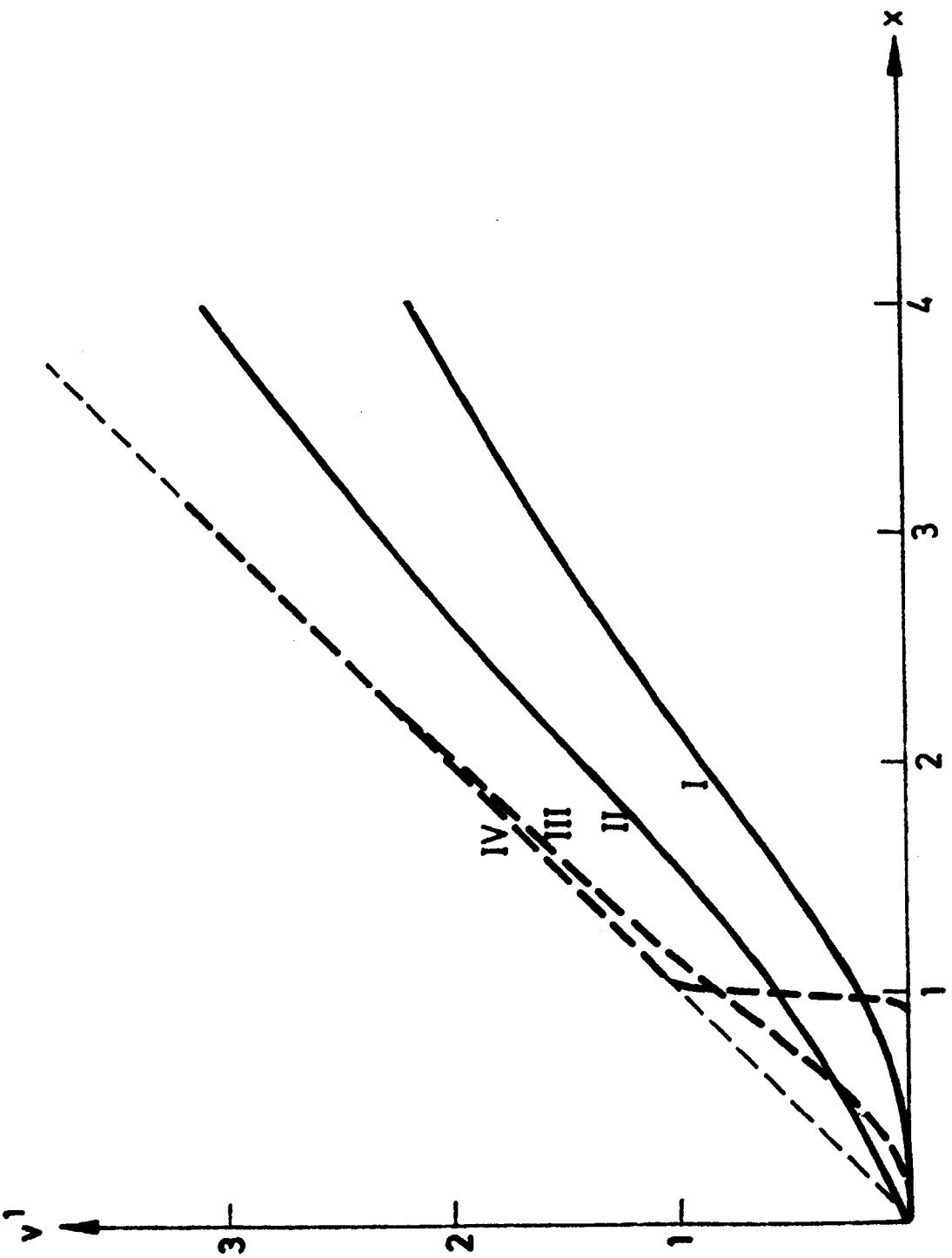

Fig. 5

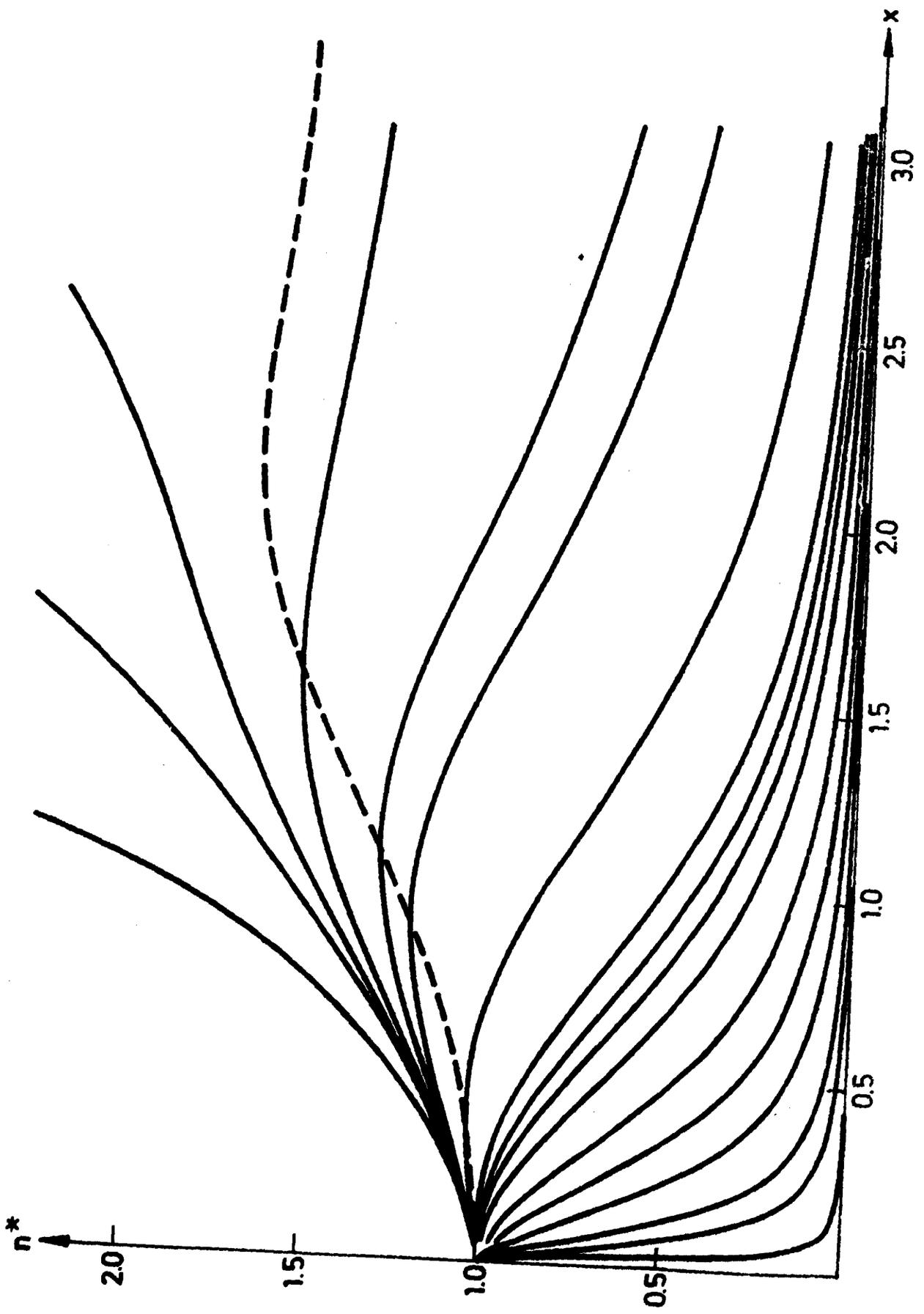

Fig. 6

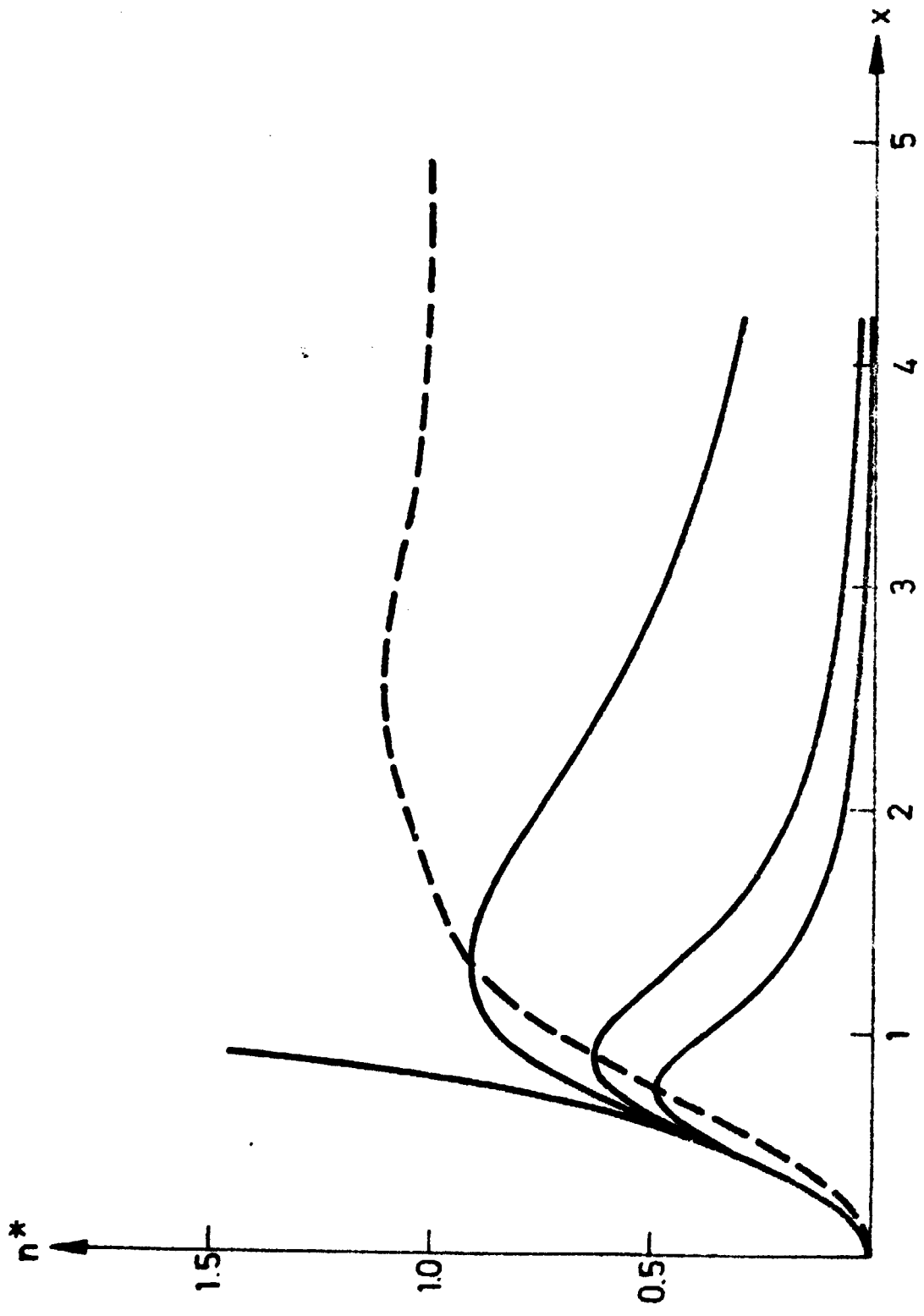

Fig. 7

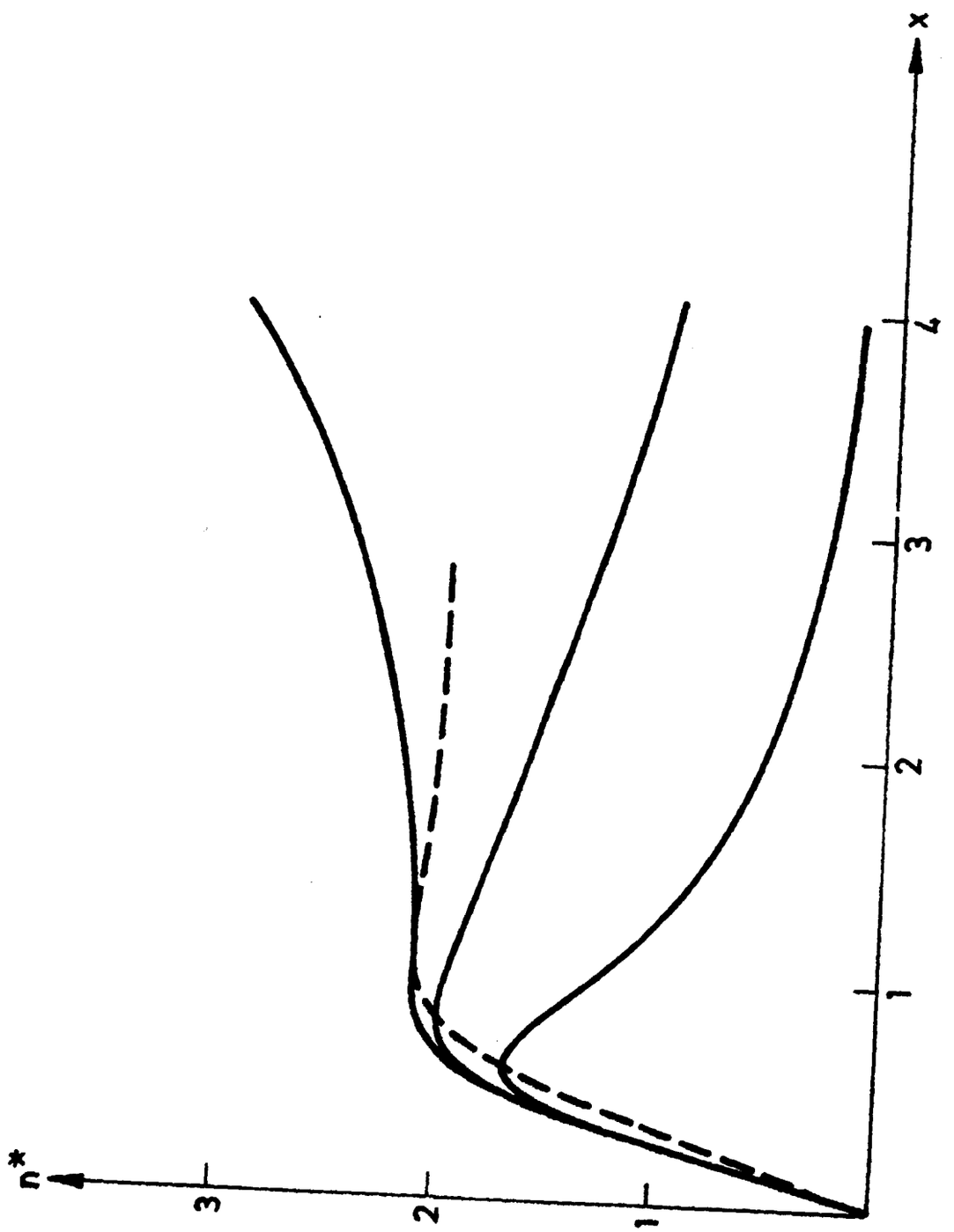

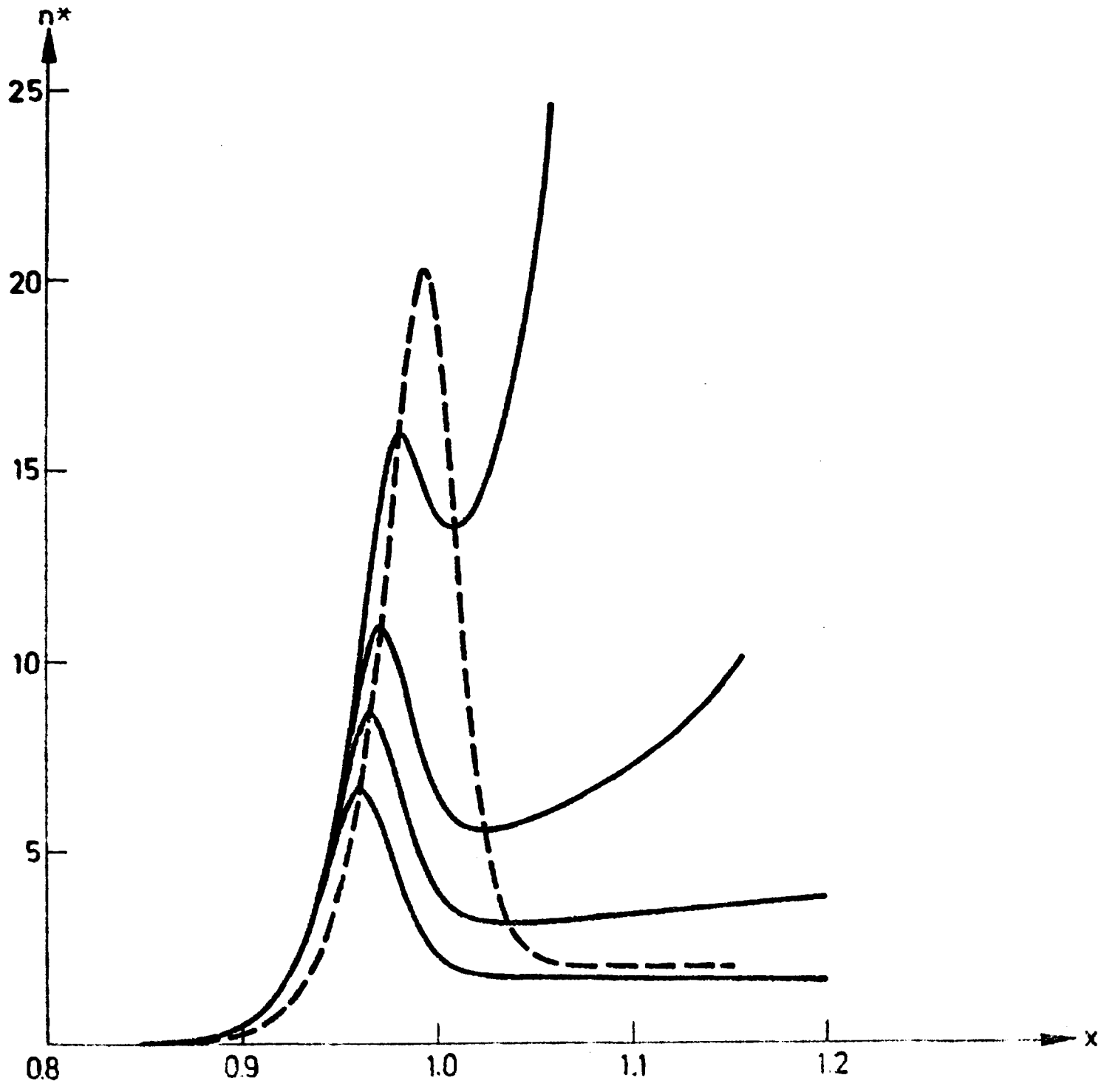
n*
25
20
15
10
5
0.8
0.9
1.0
1.1
1.2
x

Fig.9

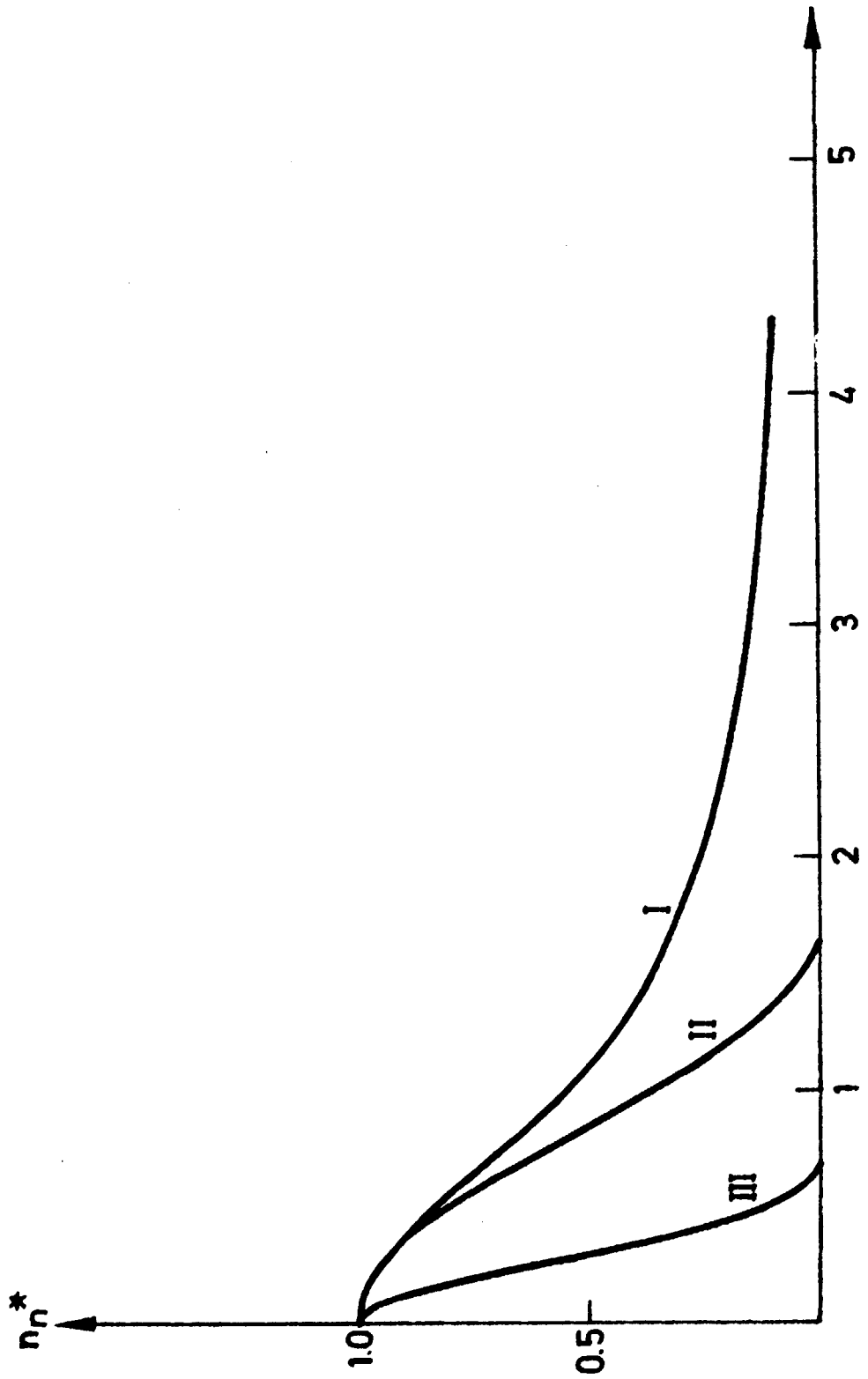

Fig. 10

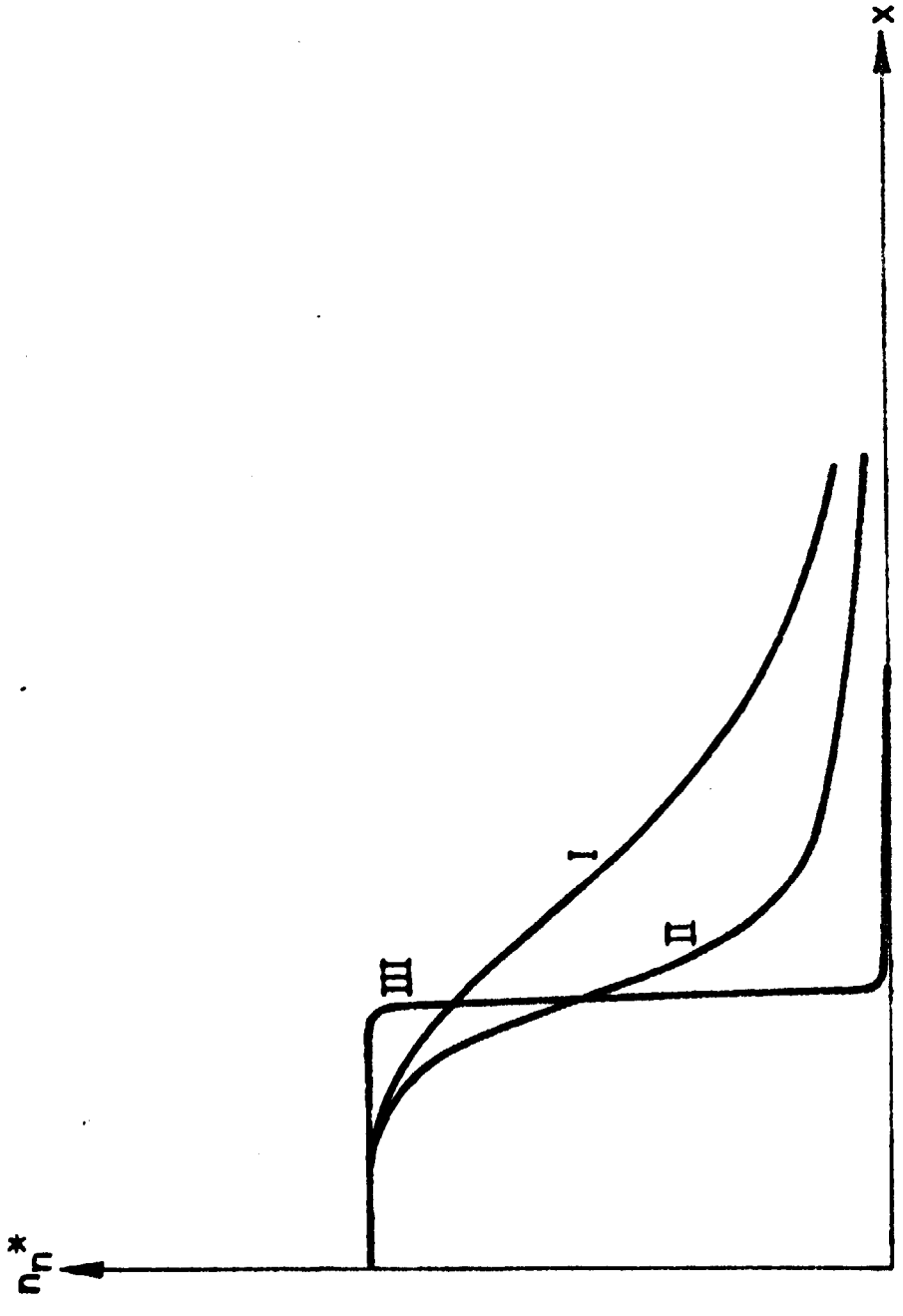

TRITA-EPP-78-09

Royal Institute of Technology, Department of Plasma Physics,
S-100 44 Stockholm, Sweden

STEADY STATE MODELS FOR FILAMENTARY PLASMA STRUCTURES ASSOCIATED WITH FORCE FREE MAGNETIC FIELDS

Göran Marklund, May 1978, 33 pp. incl. ill., in English

This paper presents a model for filamentary plasma structures associated with force-free magnetic fields. A homogenous electric field parallel to the symmetry axis of the magnetic field is assumed. Under the influence of these fields, the plasma will drift radially inwards with the velocity $v = \frac{E \times B}{B^2}$ resulting in an accumulation of plasma in the central region. We assume recombination losses to keep the central plasma density at a finite value, and the recombined plasma i.e. the neutrals to diffuse radially outwards. Plasma density and some neutral gas density distributions for a steady state situation are calculated for various cases.

Key words: Filament, Force free magnetic field, Recombination
Plasma Convection, Chemical separation